Experimental Cell Research **272,** 153–162 (2002)
doi:10.1006/excr.2001.5408, available online at http://www.idealibrary.com on IDEAL®

Fibroblast Contractile Force Is Independent of the Stiffness Which Resists the Contraction

T. M. Freyman,* I. V. Yannas,† R. Yokoo,* and L. J. Gibson*,[1]

*Department of Materials Science and Engineering and †Department of Mechanical Engineering, Massachusetts Institute of Technology, 77 Massachusetts Avenue, Cambridge, Massachusetts 02139

Using a device named the cell force monitor, the contractile force developed by fibroblasts has been studied by measuring the macroscopic contraction of porous collagen–glycosaminoglycan (GAG) matrices over the first 24 h following cell attachment. In this paper, the effect of a variation in the stiffness that resists matrix contraction by cells on the contractile force generated by the cells was determined. Data from these experiments revealed that the contractile force generated by the fibroblasts was independent of the stiffness of the resistance within the range tested (0.7–10.7 N/m). These results suggest that during the time when fibroblasts are attaching to and spreading on collagen–GAG matrices the contractile forces they generate are force limited, not displacement limited. Therefore, the cytoskeletal mechanism of force generation, corresponding with cell elongation, is capable of increasing the displacement of adhesion sites in order to develop the same level of force. Although a detailed understanding of how the passive mechanical signals provided by substrate materials affect cell processes is still unavailable, *in vitro* modeling of cell-mediated contraction continues to provide useful information.

Key Words: **wound contraction; myofibroblasts; cell forces; matrix contraction; collagen matrix; fibroblasts; stiffness; tensional homeostasis.**

INTRODUCTION

During one of the intermediate stages of dermal wound repair myofibroblasts appear in large numbers at the wound site [1]. The presence of myofibroblasts has been linked to wound contraction and extracellular matrix (ECM) synthesis associated with scar formation [1–4]. Concurrent with the differentiation of fibroblasts is an increase in the stiffness of the wound due to extracellular matrix production and remodeling processes. Along with chemical signals, it has been suggested that the higher ECM stiffness is a cue for the differentiation to myofibroblasts. After the wound has closed the density of myofibroblasts decreases and the scar tissue becomes sparsely populated by normal dermal fibroblasts as ECM remodeling slows down [1].

The use of a specific collagen–glycosaminoglycan (GAG) ECM analog, grafted onto the debrided wound bed, has resulted in the formation of a partially regenerated dermis, instead of scar tissue, apparently through blocking of wound contraction [3]. As part of the wound healing response, fibroblasts and other cells migrate into the ECM analog within the first few days and remodel it by producing new collagen and enzymes specific for ECM proteins. Interestingly, myofibroblasts thought to be responsible for wound contraction are present in wounds grafted with this ECM analog. However, culture of a fibroblast-seeded collagen–GAG matrix sample *in vitro* results in the contraction of this sample. It is not clear why *in vitro* and *in vivo* contraction phenomena diverge.

The interaction between fibroblasts and various ECM analogs which leads to contractile phenomena has been investigated *in vitro* using various methods [5–9]. Several devices have been built which allow the contractile force to be measured as a function of time [7, 10–13]. Results from some of these experiments suggest that the force generated by the fibroblasts is a homeostatic response such that an externally effected change in this force elicits a cellular response to minimize the change [7, 10, 13]. Many cellular processes, including α-smooth muscle actin production, are affected by altering the stiffness of the substrate on which the cells are cultured *in vitro* [14–16]. An understanding of the link between stiffness and fibroblast differentiation *in vitro* may lead to an explanation of the appearance and disappearance of myofibroblasts *in vivo*.

We have previously described a device, the cell force monitor (CFM), designed to measure the contractile force generated by cells seeded onto a porous matrix [17]. In this study, we report results of three sets of

[1] To whom correspondence and reprint requests should be addressed at the Department of Materials Science and Engineering, Massachusetts Institute of Technology, 77 Massachusetts Avenue, Cambridge, MA 02139. Fax: (617) 258-6275. E-mail: ljgibson@mit.edu.

0014-4827/01 $35.00

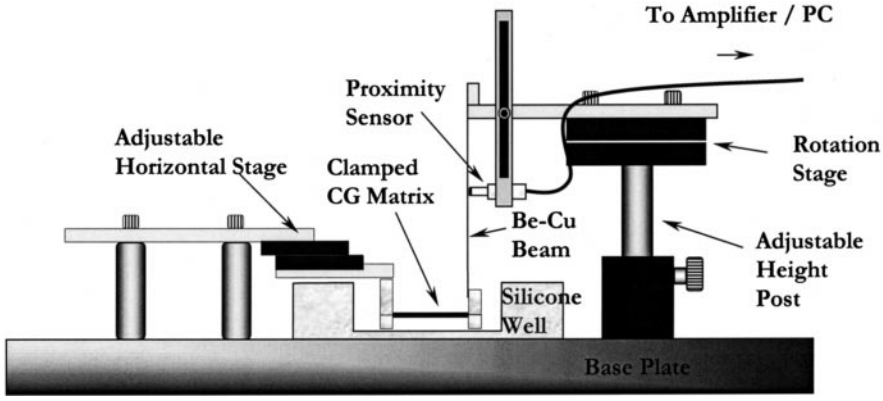

FIG. 1. Schematic of the proximity sensor cell force monitor.

experiments designed to measure the effect of the total stiffness on the contractile response of fibroblasts. First, we studied the effect of systematic variation in the beam stiffness on the short-term (22 h) force generation. Second, the elongation of the fibroblasts during the contraction in the cell force monitor was compared for two different beam stiffnesses. Finally, unrestrained, free-floating matrices with different degrees of crosslinking (and hence, matrix stiffness) were used to measure the long-term (15 day) contractile response. If the level of force generated by the fibroblasts is truly a tensionally homeostatic, or force-limited, response, the force generated per cell should be independent of the total stiffness. However, if the displacement produced per cell is independent of the total stiffness, the contractile response is displacement limited. The experiments described in this study are designed to indicate if fibroblast contraction is force limited or displacement limited. This study contributes to understanding the effect of the mechanical environment on the contractile response. As described above, characterization of the contractile response is important in understanding tissue regeneration.

METHODS

Collagen matrices. Type I collagen (Integra Life Sciences, Plainsboro, NJ) was blended at 4°C with 0.05 M acetic acid at a concentration of 5 mg/ml. A GAG, chondroitin 6-sulfate (0.44 mg/ml) (Sigma Chemical Company, St. Louis, MO) solution was added to this mixture and blended at 4°C to produce a white coprecipitate. This coprecipitate was then freeze-dried to produce a porous sheet of type I collagen and chondroitin 6-sulfate, or collagen–GAG. The resulting matrix had a pore size of ~140 μm. Matrix samples to be used in the cell force monitor experiments were subsequently crosslinked by treatment at 105°C and a vacuum of <50 torr for 24 h [3]. A second set of matrix samples, to be used in the free-floating experiments, were crosslinked for only 1 h, producing a less stiff matrix. Compressive modulus was determined for the matrix samples used in each set of experiments as described previously [17]. Rectangular samples, 50 × 28 × 3 mm, for cell force monitor experiments, and disks, 9 mm in diameter × 3 mm thick, for free-floating experiments, were cut from the fully processed matrix sheets.

Cell culture. Dermal fibroblasts were isolated from New Zealand White rabbit skin explants [17]. The fibroblasts were cultured in DMEM (GIBCO, Grand Island, NY) supplemented with 10% FBS (Hyclone Laboratories, Logan, UT), 2% penecillin/streptomycin, 1% Fungizone, and 1% L-glutamine (GIBCO). A suspension of fifth to seventh passage fibroblasts was produced for seeding the collagen–GAG matrices using trypsin–EDTA (Sigma), centrifuging, and adding the appropriate amount of culture medium. Viable cell number was determined using trypan blue and a hemacytometer.

Quantitative measurement of contraction using the cell force monitor. A CFM capable of measuring the force exerted by fibroblasts attached to a collagen–GAG scaffold was described previously [17]. Briefly, a clamped, fibroblast-seeded collagen–GAG scaffold was held fixed at one end and attached to a compliant beam on the other (Fig. 1). The previous device was modified by substituting a proximity sensor for the strain gage bridge. The proximity sensor monitored the beam deflections resulting from contraction of the scaffold by the fibroblasts without contacting the beam. This modification allowed beam stiffness to be varied, through changes in geometry, with little effort. The design of the proximity sensor/beam configuration resulted in a voltage response which was linear with beam displacement and force applied to the beam. This voltage was recorded for 22 h postseeding by a data acquisition card (AT-MIO-16XE-50; National Instruments, Austin, TX) installed in a PC (Compaq, Pentium II). Force and displacement of the beam were calculated by multiplying the recorded voltage by the appropriate calibration factors [17]. Opposing force in the matrix was calculated using the compressive stiffness of the matrix and the deflection of the beam end. The deflection of the beam end and matrix were identical so that the beam and matrix acted in parallel and the total force (defined as the sum of the forces in the beam and matrix due to the deformation) was the sum of the force in each element,

$$F_{\text{total}} = F_{\text{beam}} + F_{\text{matrix}} = V \cdot C_{\text{force}} + V \cdot C_{\text{displ}} \cdot K_{\text{matrix}}, \qquad (1)$$

where V was the voltage measured, C_{force} and C_{displ} were calibration factors for force and displacement, respectively, and K_{matrix} was the stiffness of the matrix. A complete analysis of the deflections and forces is given in [17]

In this study, the stiffness of the CFM was controlled by varying the beam geometry. Three CFMs, identical except for their beam stiffnesses, were used to measure the contractile response of the fibroblasts. The matrix stiffness was constant (0.7 ± 0.09 N/m). The three beam geometries were chosen such that the beam stiffness was negligible compared to the matrix stiffness (dimensions 150 × 10 × 0.005 mm), similar to the matrix stiffness (dimensions 90 × 10× 0.15 mm), or much higher than the matrix stiffness (dimensions 50 ×

TABLE 1

Total Stiffnesses for CFM Experiments

	Beam stiffness [N/m]	Matrix stiffness [N/m]	Total stiffness [N/m]
Stiffest CFM	10	0.7	10.7
Intermediate CFM	0.7	0.7	1.4
Least stiff CFM	3.3×10^{-6}	0.7	0.7

10×0.15 mm). Total CFM stiffness was equal to the sum of the beam and matrix stiffness (Table 1). Five tests were done in each CFM with a given beam stiffness.

After the freeze drying and crosslinking processes, specimens of the matrix material were cut to the appropriate size and rehydrated by immersion in 10 ml DMEM with 10% FBS in a tube for 10 min. A suspension of 4 million fibroblasts was then added and attachment of the fibroblasts to the matrix was facilitated by placing the tube on a rocking platform in a cell culture incubator for 10 min. Previous observations indicated that cells attached to both the top and the bottom surfaces and infiltrated to some extent into the matrix (unpublished data). We did not observe a continuous monolayer on either the top or bottom surface. Cell-seeded matrices were then carefully attached to the cell force monitors, and data acquisition was begun.

Contractile force with time data were corrected for any voltage changes not attributable to the interaction of the fibroblasts with the matrix by testing unseeded matrix samples and subtracting the average ($n = 3$) response from the cell-seeded response for each stiffness group. The corrected voltage data, calibration factors, and matrix stiffnesses were used along with Eq. (1) to obtain data for force and displacement against time. The resulting displacement vs time and force vs time curves for each experiment were normalized by attached cell number at 22 h and averaged ($n = 5$).

In addition to comparing qualitatively the average displacement and force per cell vs time curves, individual curves were characterized by fitting the data to the exponential relationship

$$d_c = d_{cell} \cdot (1 - e^{-t/\tau}) \quad \text{or} \quad F_c = F_{cell} \cdot (1 - e^{-t/\tau}), \qquad (2)$$

where d_c and F_c are the force and displacement per cell at time t, d_{cell} and F_{cell} are the asymptotic displacement and force per cell, and τ is the time constant. This relationship was fit to the data using nonlinear regression analysis giving two fitting parameters which describe each data set, d_{cell} or F_{cell} and τ. These parameters were then grouped by total system stiffness and averaged. Only one time constant was determined for each experiment since displacement and force are linearly related through stiffness. The different stiffness groups were also compared by the rate of contraction per cell (d_{cell}/τ).

Following the experiment the sample was cut from the clamps and bisected. Half of the sample was fixed in 10% neutral buffered formalin for histological analysis. The remaining half was rinsed in 37°C phosphate-buffered saline, to remove unattached cells, and then digested in a 2.0 U/ml solution of dispase (GIBCO) at 37°C. Attached cell number at 22 h postseeding was determined by counting cells in the dispase digest using a hemacytometer.

Fibroblast morphology determination. The effect of CFM stiffness on fibroblast morphology at 22 h postseeding was determined by measuring fibroblast aspect ratio in images of stained histological sections. Two groups of fibroblast-seeded matrix samples were cultured in CFMs of different stiffness for 22 h ($n = 4$). One group had a stiffness equal to that of the matrix (0.7 N/m), while the other was roughly four times greater (2.7 N/m). The samples were then cut from the clamps, fixed, embedded in glycomethacrylate (GMA), and cut into 5-μm-thin sections in the plane of the matrix sample with a microtome (Leitz 1512, Stuttgart, Germany). The thin sections were stained with hematoxylin and eosin (H&E) to reveal fibroblast morphology. A digital camera (DEI-750; Optronics Engineering) attached to a light microscope (LaboPhot; Nikon) was used to gather images from samples from both stiffness groups. The aspect ratios of at least 65 cells from each sample, for a total of approximately 280 cells per stiffness group, were measured using the particle analysis tool provided with Scion Image (http://www.scioncorp.com/). Only fibroblasts which appeared to be attached to the matrix and in which a dark, ovoid nucleus could be identified were included. The average aspect ratio for each sample was determined and then averaged with all samples in that stiffness group ($n = 4$). In addition, aspect ratio measurements from all samples of the same stiffness were plotted on a histogram to determine if total stiffness had an effect on the distribution of aspect ratios.

Free-floating experiments. The long-term effects of collagen–GAG matrix stiffness on fibroblast-mediated matrix contraction were determined by monitoring dimensional changes of free-floating disks of matrix crosslinked for either 1 or 24 h. Free-floating disks were used for two reasons. First, a majority of cell contraction research has been performed using free-floating disks, allowing comparison with previous results. Second, the CFM is not ideal for long-term contraction experiments because its design and sensitivity make it susceptible to errors associated with evaporation of medium. Disks of collagen–GAG matrix, 9 mm in diameter, were rehydrated and seeded using the same method as in the CFM experiments. Unseeded controls and fibroblast-seeded matrix disks were then floated on DMEM with 10% FBS in agarose-coated 12-well tissue culture plates. The diameter of the matrix disks was recorded on days 1, 3, 6, 7, 9, 12, 13, and 15 by comparing them to printed circles of a known diameter (± 0.5 mm).

Reduction in diameter against time for each sample was calculated by subtracting the diameter at that time point from the diameter at day 1 and deducting the average diameter change measured in the cell-free matrices over the same time period. Percentage reduction in diameter, for each sample, was determined by dividing this value by the diameter at day 1 for that sample. The average and the standard error were then determined for each time point from the individual values of percentage reduction in diameter ($n = 8$ for days 3 and 6; $n = 4$ for days 7, 11, 13, and 15). In addition, attached cell number was determined for both matrix stiffnesses at days 1, 6, and 15 ($n = 3$) by the dispase digestion method described above. On each of these days, one sample from each matrix stiffness group was fixed in 10% neutral buffered formalin and subsequently embedded in GMA. Light micrographs, from H&E-stained GMA sections, were gathered to compare qualitatively changes in fibroblast distribution and matrix microstructure with time.

Statistical methods. A two-tailed, heteroscedastic Student t test was used to determine the significance of the effect of stiffness on cell number at 22 h postseeding, fibroblast aspect ratio in CFM experiments, and matrix diameter at various days postseeding in free-floating experiments. Two-way ANOVA was used to determine the significance of the effects of time and crosslink treatment on cell number in free-floating samples.

RESULTS

Matrix Compression

Plots of engineering stress vs strain show that mechanical behavior of the collagen–GAG matrix was linear ($R^2 > 0.93$) up to the highest imposed strains, 20%. Modulus values for the matrices used in the free-floating experiments were 19 ± 4.4 Pa ($n = 6$) and

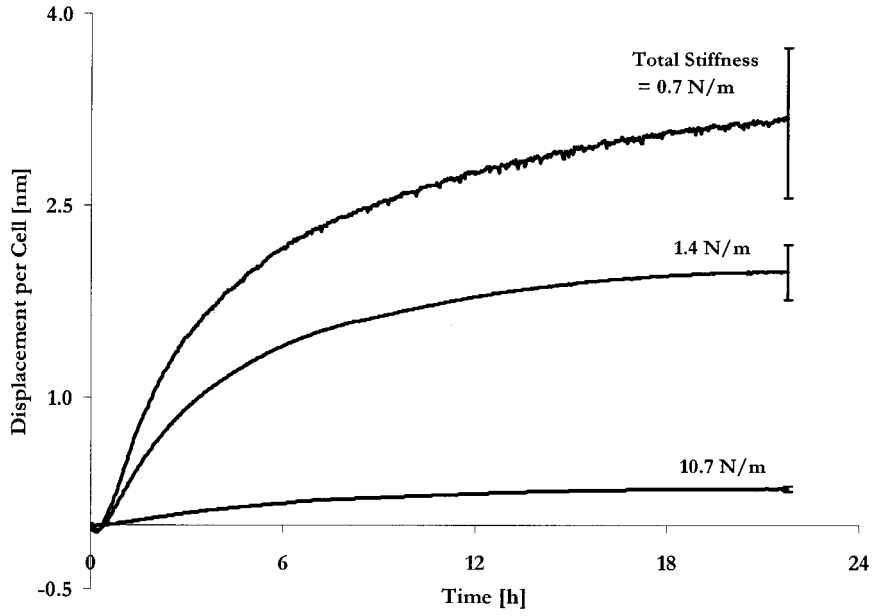

FIG. 2. Plot of displacement per cell over time for different total stiffnesses. The displacement developed per cell increased as the total stiffness decreased.

54 ± 9 Pa (n = 5) for the 1- and 24-h crosslinking groups, respectively, for a modulus ratio of 2.8. The matrix samples used in the CFM experiments, which were crosslinked for 24 h, had a modulus of 47 ± 5.9 Pa (n = 11).

Quantitative Contraction Measurement Using the CFM

Contraction experiments using the CFM provided a time-continuous measurement of matrix displacement from which average displacement and force per cell were calculated for three different levels of total stiffness (defined as the sum of the stiffness of the beam and the matrix). Displacement and force per cell increased with time, approaching an asymptotic level by ~15 h postseeding for all total stiffnesses (Figs. 2 and 3). A plot of displacement per cell against time showed that the asymptotic level was lower for higher values of total stiffness (Fig. 2). In contrast, a plot of force per cell against time showed similar asymptotic levels for

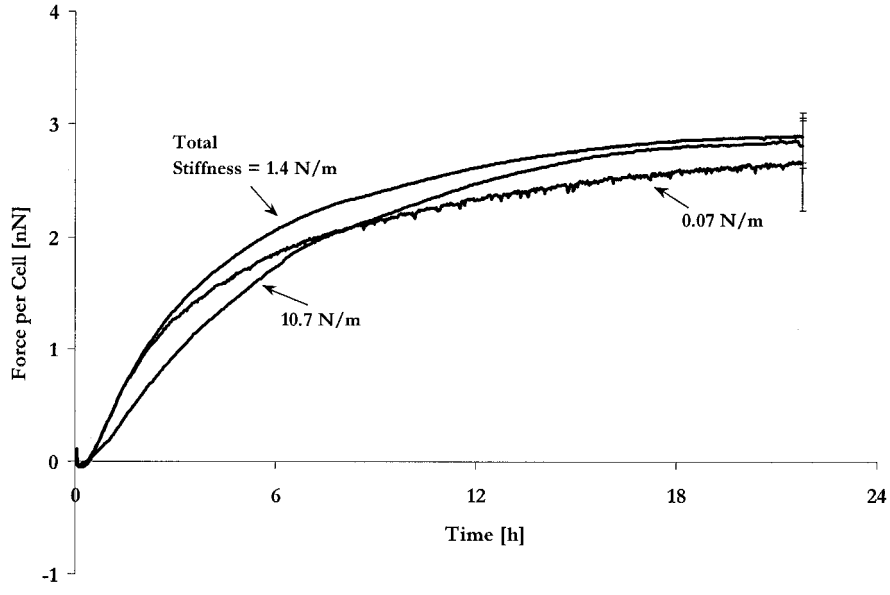

FIG. 3. Plot of force per cell over time for different total stiffnesses. The force developed per cell was independent of the total stiffness.

TABLE 2

Exponential Curve Fit Parameters

Curve fit parameters	Total stiffness [N/m] 10	1.4	0.7
Mean asymptotic displacement per cell, d_{cell} (nm)	0.32 ± 0.03	2.0 ± 0.2	3.2 ± 0.6
Mean asymptotic force per cell, F_{cell} (nN)	3.2 ± 0.3	2.9 ± 0.2	2.7 ± 0.4
Mean time constant, τ (h)	7.9 ± 1.3	5.2 ± 0.85	5.1 ± 0.60
Characteristic rate of contraction per cell (d_{cell}/τ) (nm/(h · cell))	0.04 ± 0.004	0.4 ± 0.04	0.62 ± 0.06

all total stiffnesses (Fig. 3). There was no significant effect ($P > 0.4$) of total stiffness on the number of attached cells at 22 h, approximately 900,000 cells per CFM sample.

The curve fit parameters, d_{cell}, F_{cell}, and τ, resulting from fitting Eq. (2) to the data in the plots of displacement and force per cell against time are reported in Table 2. All curve fits resulted in a high correlation with the data, $R^2 > 0.98$. The total stiffness had a significant effect ($P = 0.0006$) on the asymptotic value of displacement per cell, d_{cell}, and had no significant effect ($P = 0.6$) on the asymptotic force per cell, F_{cell}, ~3 nN. The time constant, τ, is a measure of how quickly the displacement or force develops. The average time constant for the stiffest system (7.9 h) was not statistically different ($P > 0.1$) from those for the two lower stiffness systems (5.2 and 5.1 h) (Table 2). The rate at which each cell contracted (Table 2) was also affected by the total stiffness; the fibroblasts contracted the less stiff systems more rapidly.

Aspect Ratio Comparison

To determine if fibroblasts altered their morphology in order to increase the amount of displacement per cell, the average and frequency distribution of fibroblast aspect ratios at 22 h postseeding for the two total stiffnesses were determined. The average aspect ratios of fibroblasts in the compliant and stiff systems, 2.3 and 2.1 ± 0.15, respectively, were not statistically different ($P = 0.39$). The distribution of aspect ratios was also similar for both stiffnesses (Fig. 4). Half of the fibroblasts were only slightly elongated (aspect ratio <2) after 22 h. The remainder of fibroblasts appeared to have elongated (aspect ratio >2), with some aspect ratios as high as 7.

Free-Floating Matrix Contraction

Fibroblast-mediated contraction of free-floating collagen–GAG matrix disks was significantly greater in the more compliant matrix at all time points ($P < 0.007$) (Fig. 5). The largest difference, 10%, occurred within the first 3 days. During this time the diameter of stiffer matrix disks did not change significantly from day 1 ($P = 0.1$). For the lower stiffness matrix, the percentage reduction in diameter per day, ~4%, was similar up through day 6. Between days 6 and 7, the percentage reduction in diameter per day de-

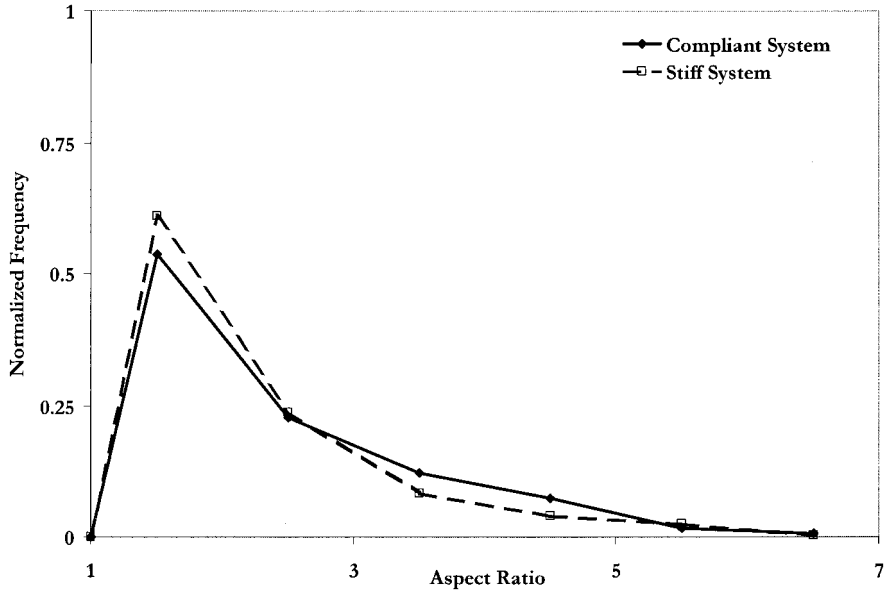

FIG. 4. Histogram showing the distribution of aspect ratios at 22 h postseeding for cells cultured under two different total stiffnesses.

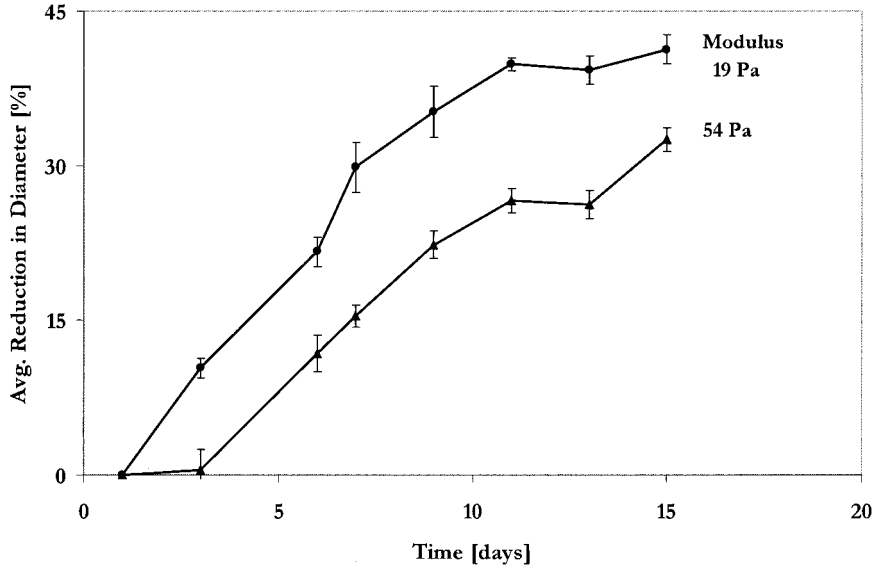

FIG. 5. Plot showing the effect of initial matrix stiffness on the average reduction in diameter of free-floating matrix disks over 2 weeks in culture. The attached cell number does not vary significantly with time or between initial stiffness groups.

creased to 8 from 4%. Beyond this point diameter reduction slowed; after the 11th day there was no statistically significant change ($P > 0.2$) in the diameter. After the initial lag and up to day 11, the diameter of the stiffer matrices was reduced by a rate, ~3%, similar to that observed in the less stiff matrices. Between days 11 and 13, no noticeable diameter reduction was recorded; however, after day 13 contraction resumed at a rate of 3% per day. The average rate of contraction, defined by the slope of a straight line fit to the data, after day 3 was similar for both stiff and compliant matrices (2% per day). The attached cell number, 139,000 fibroblasts per disk, was not significantly affected by time in culture or crosslinking treatment ($P > 0.3$).

Qualitative image analysis of H&E-stained GMA sections showed a similar distribution of fibroblasts and matrix microstructure for both matrix stiffnesses at 1 day postseeding (Fig. 6). By day 6, the pore diameter and fraction of void space had decreased noticeably in the less stiff matrices. By day 15, fibroblasts in the interior of the less stiff disks appeared to be completely surrounded by matrix with no discernable pore structure and a one-cell-thick layer of fibroblasts was present on the outside edge. In contrast, after 6 days the stiffer matrices showed no obvious pore diameter reduction. By day 15 there was a noticeable change in the pore diameter and fraction of void space. The collagen–GAG fibers appeared to have swelled more for the less stiff matrix samples by day 6, contributing to reduction in void space. No detailed analysis of this phenomenon was pursued.

DISCUSSION

Asymptotic Contractile Force Is Independent of Total Stiffness of CFM and Matrix

The results of this study give a clear demonstration of the effect of the mechanical environment on the contractile response of fibroblasts and, so, of the mechanosensing ability of fibroblasts. The quantitative results show that fibroblasts contract the substrate to attain a particular value of force per cell rather than a particular value of displacement per cell. Contraction proceeded until an asymptotic force of ~3 nN per cell was reached, regardless of displacement per cell (0.3–3 nm). The value of asymptotic force per cell, F_{cell}, is comparable to the value of 1 nN reported previously for a similar system [17]. These previous experiments showed that the total force developed by all cells in the collagen–GAG matrix sample was dependent on the number of cells, but F_{cell} and τ remained constant. The discrepancy in the value of F_{cell} could be due to the use of a different fibroblast seeding technique, lot of serum, and matrix sample size. We can now conclude for this system that the force per cell and the time constant for the development of the force are independent of the total number of cells and the total stiffness of the system. The contractile displacement, on the other hand, increases inversely with the system stiffness.

This study is the first to use an experimental system in which the system stiffness could be varied and quantified. Previous studies have measured the contractile response of fibroblasts on collagen gels of varying concentration, but were not able to characterize the stiff-

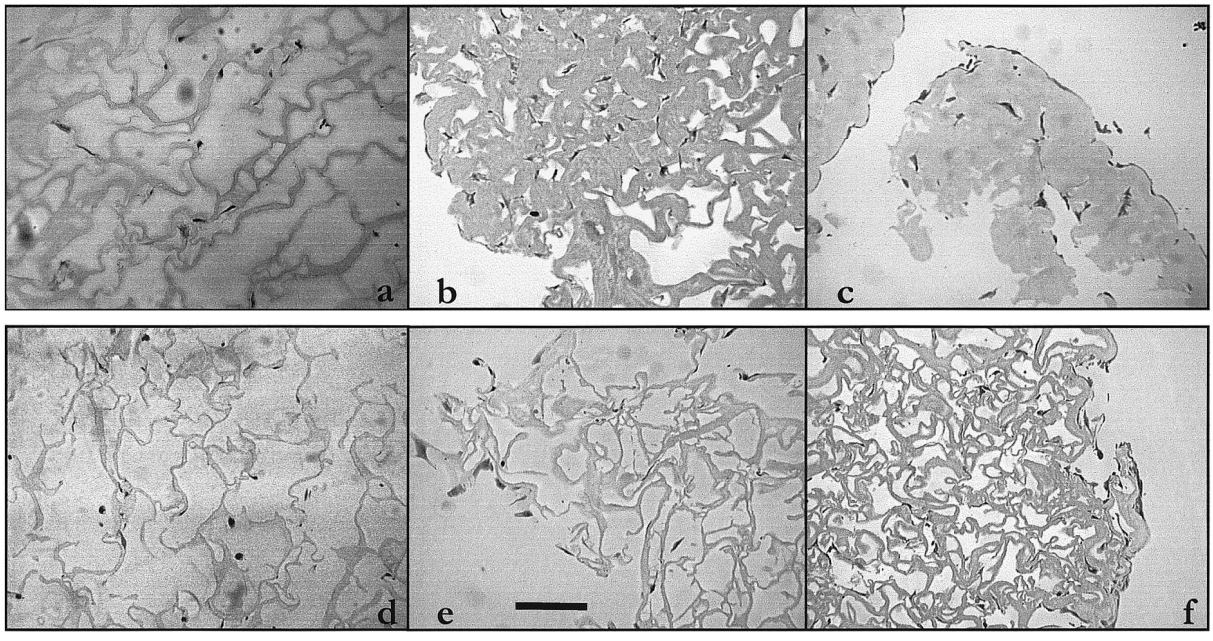

FIG. 6. Light micrographs of H&E-stained GMA sections of free-floating matrix samples showing cell distribution and matrix microstructure changes with time. Less stiff matrix disks are shown in a, b, and c for time points 1, 6, and 15 days, respectively. Stiffer matrix disks are shown in d, e, and f for time points 1, 6, and 15 days, respectively. Scale bar, 200 μm

ness of the gels directly. One study [10], using anchored collagen gels populated with fibroblasts, showed an increase in contractile force with an increase in concentration of collagen gel while another [18], using free-floating collagen gels populated with fibroblasts, reported a decrease in overall contraction with increasing collagen concentration. The lack of quantitative microstructural and stiffness data characterizing the gels in these studies, as well as the difference in the constraint (anchored vs free floating), makes interpretation of their apparently contradictory results difficult.

There is substantial evidence that contractile cells are largely responsible for spontaneous closure of injuries in a large number of organs in adults, including the skin, the peripheral nerves, the ureter, the ligament, the urethra, the esophagus, and the upper eyelid. There is additional evidence that selective blocking of contractile cells in skin, peripheral nerves, and the conjunctiva leads to partial regeneration of the severely injured organ in each case [19]. Characterization of the contractile response of cells is therefore important in understanding tissue regeneration. This study contributes to understanding the effect of the mechanical environment on the contractile response.

Contractile cells (myofibroblasts) become differentiated from fibroblasts when certain critical conditions are present. These conditions include not only the presence of certain cytokines, such as TGF-β1, in the serum but also the mechanical state of the cells [1]. Previous investigators have found that the stiffness of collagen gels regulates TGF-β1 induction of α-SMA in fibroblasts, with increased gel restraint increasing the production of α-SMA in response to TGF-β_1 [16]. The results of the present study indicate that fibroblasts contract the substrate to attain a particular value of force per cell; there is, however, insufficient evidence on which to conclude that this force level corresponds to the mechanical state required for the differentiation process referred to above. In addition to effects on cell processes, the linkage between integrins and the cytoskeleton was found to strengthen in response to an increase in the extracellular matrix's ability to resist cellular forces [15, 20].

Force Generation Approaches a Homeostatic Level

Previous studies have shown that fibroblasts acted to minimize externally imposed changes from the asymptotic level of force [7, 10, 13]. This behavior, termed tensional homeostasis [13], was interpreted to be a negative feedback loop through which the cell actively tries to maintain a particular level of force in the substrate. Data presented in this paper show that the level of force which satisfies the homeostatic criterion is likely to be independent of the stiffness of the substrate. The fibroblasts maintained a very similar force in the matrix at all times postseeding regardless of the amount or rate of deformation required (Table 2). In our previous work [21] and in results reported by other

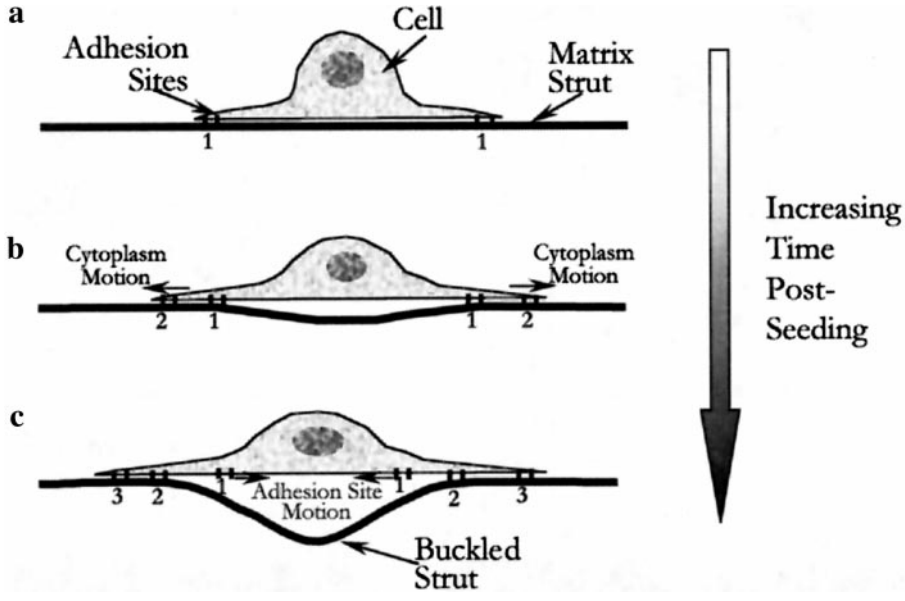

FIG. 7. Schematic showing the centripetal motion of adhesion sites and the centrifugal motion of cytoplasm. This attempts to explain the phenomenon of simultaneous cell elongation and matrix contraction. (a) As the cell elongates, due to cytoplasm motion, new adhesion sites form near the leading edge. (b) Adhesion sites (1) move centripetally, and new adhesion sites form (2) at the leading edge of the elongating cell. The matrix strut buckles due to the force generated by the cell. (c) The adhesion sites (1) have detached from the matrix strut as they near the cell center and the matrix strut moves away as it deforms. Adhesion sites (3) continue to form at the leading edge of the elongating cell, and established adhesion sites moving centripetally further deform the strut.

investigators [14] cell spreading was adversely affected when cells were seeded onto a very compliant substrate. If our hypothesis linking cell elongation with matrix contraction is correct, this would have resulted from the substrate not providing enough mechanical resistance (or support) to allow for proper spreading. The homeostatic response to external factors [13] would then have been a reaction by the cell to reestablish its morphology.

The Cellular Mechanism of Matrix Contraction

It was previously shown [21] that the force measured in the CFM was linked to cell elongation. Results presented in this paper showed that changing the total stiffness did not affect the level of force developed by fibroblasts; therefore, displacement per cell increased with decreasing total stiffness. This suggests either that the development of force through cell elongation was a force-limited process or else that individual cells generated larger displacements, within the same time period, in order to attain the same level of force.

Elongation was observed to occur through a spreading and thinning of the fibroblast's cytoplasm [21]. The deformation observed in struts in the matrix suggested that as cells elongate, adhesion sites form at the leading edge and likely release near the cell center. The compressive contraction of a strut under an elongating cell is counterintuitive. A possible explanation for this phenomenon is the simultaneous centripetal movement of adhesion sites and centrifugal movement of cytoplasm (Fig. 7). The centripetal movement of adhesion sites in stationary cells has been described previously [22]. Therefore, the increase in strut deformation which was observed suggested that the centripetal motion of adhesion sites occurred until a particular level of extracellular force was reached. The mechanics of matrix strut deformation can be explained by analogy with the force balance in a simple three-member truss. Tensile forces in the bracing members of a truss (analogous to the actin fibers in the cell) induce compression in the bottom chord (analogous to the matrix strut). As the cells elongate, and adhesion sites form at the periphery of the cell and release near the cell center, the length of the matrix strut under compressive load increases, decreasing the load required to buckle the strut. In some cases, as the cell elongated, the compressive load applied to the matrix strut by the cell was sufficient to buckle the matrix strut [21].

The time constant defining the development of matrix contraction in the CFM was not dependent on the total stiffness, but the rate at which displacements were generated per cell was dependent on the total stiffness (Table 2). Previously, the time dependence of matrix contraction in the CFM was explained by the stochastic nature of cell elongation initiation and the time required for each cell to reach a final elongated state [21]. Individual cells were observed to reach a final deformation state within ~2–4 h, while the popu-

lation–averaged elongation and contraction in the CFM took ~15 h. The independence of the time constant for CFM experiments with varying system stiffness suggested that the process just described was not sensitive to the external resistance (stiffness) provided. However, the similarity in time constants and large differences in value of displacement per cell indicated that individual cells deformed the matrix more rapidly when cultured in the less stiff system. Therefore, not only was the mechanism of matrix deformation associated with cell elongation limited by the force, it was also capable of developing larger displacements at faster rates to maintain the same time constant.

Fraction of Fibroblasts Participating in Contraction

The above arguments assume that the fraction of cells which participated in the contraction of the collagen–GAG matrices did not vary with changes in total stiffness. Force and displacement numbers were normalized by the number of attached fibroblasts at the termination of the contraction experiments. It is possible that only a fraction of the attached fibroblasts actively participated in the contraction. This can be explained by differences in the cell cycle, by localized variations in stimuli, or by differences in cell–cell proximity. The aspect ratio or amount of cell elongation is an indication of a fibroblast's contractile activity *in vitro*. The observation of fibroblasts which have not elongated significantly, with aspect ratios less than 1.2 after 22 h in culture (Fig. 4), is evidence for the presence of inactive fibroblasts. However, the similarity in the average aspect ratio and in the distribution of aspect ratios (Fig. 4) for a four-fold difference in total stiffness suggests that the fraction of active cells was not affected by the total stiffness.

Matrix Stiffness Affects Contraction Occurring over Several Days

The contraction of free-floating, fibroblast-seeded, collagen–GAG matrices was greater for less stiff matrices after 15 days in culture (Fig. 5). This contraction can be divided into three phases: lag, steady contraction, and slowing contraction. The presence of the lag phase for stiffer matrices is consistent with previously reported results [23]. The majority of contraction occurs in the steady contraction phase, prior to day 11 in culture. After this phase, the less stiff matrices had contracted 50% more than the stiffer matrices. Compared to the 300% increase in stiffness, there does not seem to be a simple linear relationship between initial stiffness and long-term, unrestrained contraction. This result is not entirely unexpected since changes in crosslink density affect matrix properties other than stiffness (e.g., degree of collagen swelling).

A similar decrease in contraction of tenocyte-seeded collagen–GAG matrices with an increase in crosslinking was observed previously [23]. In this case, a linear relationship ($R^2 > 0.7$) was established between the contraction at 21 days, normalized by DNA content, and the tensile modulus of the collagen–GAG matrices over a much larger range of stiffness using several different crosslinking treatments. Although experimental configurations of this type do not provide a clear link between contraction and matrix stiffness, this result does provide insight into the long-term contractile behavior of fibroblasts in matrices with different initial stiffness.

The increase in contraction with a decrease in initial matrix stiffness in the free-floating contraction experiments is consistent with the independence of force per cell from total stiffness in the CFM experiments. However, the curves of force with time from the CFM experiments shows a trend toward an asymptotic value of force per cell. This conclusion seems to contradict the continued contraction of the free-floating matrices over several weeks. If the asymptotic level of force is actually a value which the cells attempt to attain, the continued contraction could be explained by the free-floating matrices' inability to provide sufficient resistance to contraction coupled with the continued decrease in resistance due to degradation. In addition, the difference in the mechanical stress state due to the restraint of the matrix with the clamps in the CFM also makes direct comparisons difficult.

SUMMARY

The level of contractile force generated by fibroblasts, while they are elongating on collagen–GAG substrates, is not dependent on the amount of resistance to contraction (i.e., total stiffness—the sum of the beam and matrix stiffness). This demonstrates that fibroblast contraction is a force-limited behavior, not a displacement-limited behavior. Cell elongation is occurring simultaneously with the development of this force and has the same independence from total stiffness within the range tested. Therefore, the cytoskeletal mechanism of force generation, occurring coincident with cell elongation, is capable of increasing the displacement of adhesion sites in order to develop the asymptotic level of force. Although a detailed understanding of how the passive mechanical signals provided by substrate materials affect cell processes is still unavailable, *in vitro* modeling of cell-mediated contraction continues to provide useful information.

This work was supported in part by a NIH training grant through the Department of Materials Science and Engineering at MIT and the Harvard Dental School, NIH Grant DE 13053, and the Matoula S. Salapatas Professorship in the Department of Materials Science and Engineering at MIT. We are grateful for insightful discussions with Dr. Myron Spector of the Brigham and Women's Hospital and the Harvard Medical School.

REFERENCES

1. Grinnell, F. (1994). Fibroblasts, myofibroblasts, and wound contraction. *J. Cell Biol.* **124,** 401–404.
2. Gabbiani, G., Hirschel, B. J., Ryan, G. B., Statkov, P. R., and Majno, G. (1972). Granulation tissue as a contractile organ: A study on structure and function. *J. Exp. Med.* **135,** 719–734.
3. Yannas, I. V., Lee, E., Orgill, D. P., Skrabut, E. M., and Murphy, G. F. (1989). Synthesis and characterization of a model extracellular matrix that induces partial regeneration of adult mammalian skin. *Proc. Natl–Acad. Sci. USA* **86,** 933–937.
4. Rudolph, R., Berg, J., and Ehrlich, H. (1992). Wound contraction and scar contracture. *In* "Wound Healing: Biochemical and Clinical Aspects" (I. K. Cohen, R. F. Diegelmann, and W. J. Lindblad, Eds.), Saunders, Philadelphia.
5. Roy, P., Petroll, W. M., Chuong, C. J., Cavanagh, H. D., and Jester, J. V. (1999). Effect of cell migration on the maintenance of tension on a collagen matrix. *Ann. Biomed. Eng.* **27,** 721–730.
6. Eastwood, M., McGrouther, D. A., and Brown, R. A. (1998). Fibroblast responses to mechanical forces. *Proc. Inst. Mech. Eng. Part H* **212,** 85–92.
7. Jenkins, G., Redwood, K. L., Meadows, L., and Green, M. R. (1999). Effect of gel reorganization and tensional force on alpha2beta1 integrin levels in dermal fibroblasts. *FEBS Lett.* **263,** 93–103.
8. Chapuis, J.-F., Lucarz-Bietry, A., Agache, P., and Humbert, P. (1996). A mechanical study of tense collagen lattices. *Eur. J. Dermatol.* **6,** 56–60.
9. Roy, P., Petroll, W. M., Cavanagh, H. D., Chuong, C. J., and Jester, J. V. (1997). An *in vitro* force measurement assay to study the early mechanical interaction between corneal fibroblasts and collagen matrix. *Exp. Cell Res.* **232,** 106–117.
10. Delvoye, P., Wiliquet, P., Leveque, J.-L., Nusgens, B. V., and Lapiere, C. M. (1991). Measurement of mechanical forces generated by skin fibroblasts embedded in a three-dimensional collagen gel. *J. Invest. Dermatol.* **97,** 898–902.
11. Kolodney, M. S., and Wysolmerski, R. B. (1992). Isometric contraction by fibroblasts and endothelial cells in tissue culture: A quantitative study. *J. Cell Biol.* **117,** 73–82.
12. Eastwood, M., McGrouther, D. A., and Brown, R. A. (1994). A culture force monitor for measurement of contraction forces generated in human dermal fibroblast cultures: Evidence for cell–matrix mechanical signalling. *Biochim. Biophys. Acta* **1201,** 186–192.
13. Brown, R. A., Prajapati, R., McGrouther, D. A., Yannas, I. V., and Eastwood, M. (1998). Tensional homeostasis in dermal fibroblasts: Mechanical responses to mechanical loading in three-dimensional substrates. *J. Cell Physiol.* **175,** 323–332.
14. Pelham, R. J. J., and Wang, Y.-L. (1997). Cell locomotion and focal adhesions are regulated by substrate flexibility. *Proc. Natl. Acad. Sci. USA* **94,** 13661–13665.
15. Chicurel, M. E., Chen, C. S., and Ingber, D. E. (1998). Cellular control lies in the balance of forces. *Curr. Opin. Cell. Biol.* **10,** 232–239.
16. Arora, P. D., Narani, N., and McCulloch, C. A. G. (1999). The compliance of collagen gels regulates transforming growth factor-β induction of α-smooth muscle actin in fibroblasts. *Am. J. Pathol.* **154,** 871–882.
17. Freyman, T. M., Yannas, I., Yokoo, R., and Gibson, L. (2001). Fibroblast contraction of a collagen–GAG matrix. *Biomaterials* **22,** 2883–2891.
18. Bell, E., Ivarsson, B., and Merrill, C. (1979). Production of a tissue-like structure by contraction of collagen lattices by human fibroblasts of different proliferative potential *in vitro. Proc. Natl–Acad. Sci. USA* **76,** 1274–1278.
19. Yannas, I. V. (2001). "Tissue and Organ Differentiation in Adults," Springer-Verlag, New York.
20. Choquet, D., Felsenfeld, D. P., and Sheetz, M. P. (1997). Extracellular matrix rigidity causes strengthening of integrin–cytoskeletal linkages. *Cell* **88,** 39–48.
21. Freyman, T. M., Yannas, I. V., Pek, Y.-S., Yokoo, R., and Gibson, L. J. (2001). Micromechanics of fibroblast contraction of collagen–GAG matrix. *Exp. Cell Res.* **269,** 140–153.
22. Smilenov, L. B., Mikhailov, A., Pelham, R. J., Marcantonio, E. E., and Gundersen, G. G. (1999). Focal adhesion motility revealed in stationary fibroblasts. *Science* **286,** 1172–1174.
23. Schulz-Torres, D., Freyman, T. M., Yannas, I. V., and Spector, M. (2000). Tendon cell contraction of collagen–GAG matrices *in vitro*: Effect of cross-linking. *Biomaterials* **21,** 1607–1619.

Received June 21, 2001
Revised version received October 15, 2001
Published online December 6, 2001